MASPRM: Multi-Agent System Process Reward Model

Milad Yazdani^{1*}, Mahdi Mostajabdaveh^{2†}, Zirui Zhou², Ying Xiong²

¹Department of Electrical and Computer Engineering, University of British Columbia, Vancouver, BC V6T1Z4, Canada

²Huawei Technologies Canada, Burnaby, BC V5C6S7, Canada

Correspondence: mahdi.mostajabdaveh1@huawei.com

Abstract

Practical deployment of Multi-Agent Systems (MAS) demands strong test-time performance, motivating methods that guide inference-time search and selectively spend compute to improve quality. We present the Multi-Agent System Process Reward Model (MASPRM). It assigns per-action, per-agent values to partial inter-agent transcripts and acts as an inferencetime controller. MASPRM is trained from multi-agent Monte Carlo Tree Search (MCTS) rollouts without requiring step-level human annotations, by propagating returns to local targets. At inference, MASPRM guides steplevel beam search and MCTS, focusing computation on promising branches and pruning early. On GSM8K and MATH, MASPRMguided decoding with an outcome reward model (ORM) applied to the final answer, improves exact match (EM) over a single straightthrough MAS pass by +30.7 and +22.9 points, respectively. A MASPRM trained on GSM8K transfers zero-shot to MATH without retraining, adding 8.4 EM points at the same budget. MASPRM is a plug-in value model that estimates per-agent progress and complements verifier-style decoders, enabling more reliable, compute-aware multi-agent reasoning. Code: https://github.com/milad1378yz/ **MASPRM**

1 Introduction

Large language models (LLMs) have made multistep problem solving increasingly practical. However, reliability still drops when a single pass must explore alternatives, justify choices, and coordinate subtasks (Zhang et al., 2024). Multi-Agent Systems (MAS) offer a different stance: multiple specialized agents converse over a communication graph, cross-check one another, and decompose

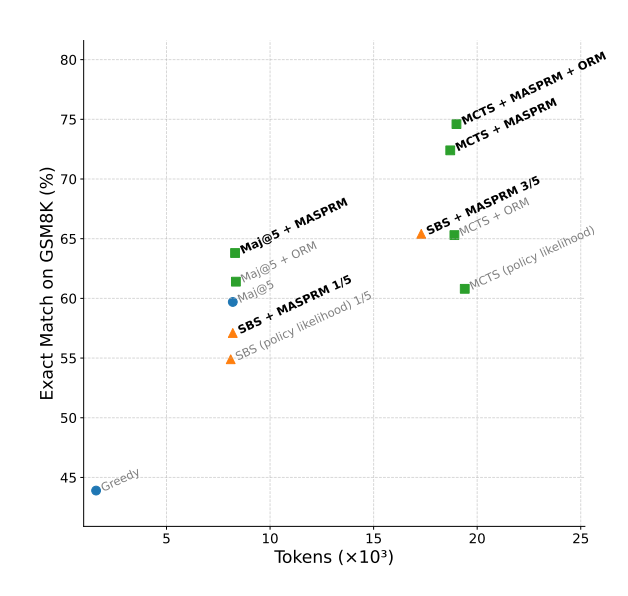


Figure 1: Token-accuracy trade-off on GSM8K. Each point reports exact match (y-axis) versus average test-time tokens (x-axis; $\times 10^3$). MASPRM consistently shifts the frontier upward: it improves Maj@5 and stepwise beam search (SBS) under matched budgets, and when paired with MCTS and an ORM, it reaches 74.6% EM at ~ 19 k tokens, while Greedy sits near 43.9% EM at ~ 1.6 k tokens.

work so that no single context or policy bears the entire burden. When paired with structured exploration and deliberation, such collaboration can outperform single-shot prompting by distributing computation across complementary roles (Wang et al., 2022; Yao et al., 2023). In parallel, the community has learned that *how* we spend test-time compute often matters more than *how many* parameters we have: procedures that expand, verify, and rank partial solutions yield substantial gains in correctness and calibration (Snell et al., 2024; Cobbe et al., 2021; Lightman et al., 2023).

Despite this promise, the inference-time search in MAS remains unreliable for two main reasons. **First,** outcome-only evaluation (e.g., majority vote or final-answer verifiers) is too sparse to steer long

^{*}Intern at Huawei Technologies Canada during this work †Corresponding Author



Inference: MASPRM-Guided Decoding

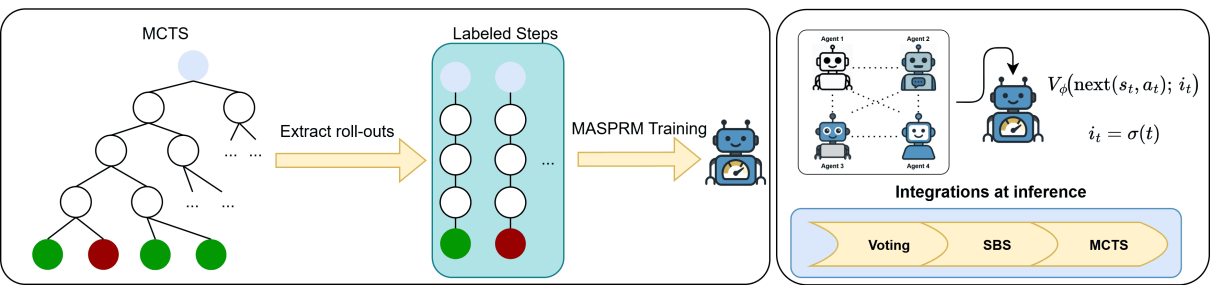


Figure 2: **Search-generated supervision.** Left: Extracted rollouts yield edge-level estimates $\hat{Q}(s,a)$; for each child s' = next(s,a) we set the regression target $y = \hat{Q}(s,a)$ and train the MASPRM $V_{\phi}(s')$ accordingly. Right: Uses of MASPRM in multi-agent systems, including inference-time guidance (SBS and MCTS via V_{ϕ} and \hat{Q}).

inter-agent exchanges; it provides little information about *which* message, from *which* agent, moved the system closer to a solution (Cobbe et al., 2021). **Second,** errors propagate across turns; without a mechanism that scores intermediate states, MAS tends to keep extending unpromising branches simply because they are likely under the policy, not because they are helpful. Prior work in single-agent settings shows that progress-aware feedback can guide inference-time search to where improvement is most likely (Setlur et al., 2024; Lightman et al., 2023; Chen et al., 2024; Guan et al., 2025; Zeng et al., 2025). However, directly transplanting these ideas to MAS is non-trivial.

We introduce MASPRM, a Process Reward Model (PRM) for Multi-Agent Systems. MASPRM estimates the value of an intermediate inter-agent state. It serves as a value head over agents' outputs, producing per-action, per-agent scores that serve two roles: (i) an inference time controller that guides expansion and early stopping over agent rollouts, and (ii) a per-agent progress signal for analysis and improving MAS. Conceptually, MASPRM transforms a long, entangled dialogue into a sequence of value-estimated actions at the agent-level, enabling MAS to allocate compute to promising branches rather than to long but unproductive ones.

Developing PRMs for MAS presents challenges beyond traditional PRMs for single-agent reasoning chains. **Granular steps and substeps.** In a single-agent chain-of-thought, a "step" typically corresponds to a small reasoning act. In MAS, a single turn expands into multiple substeps (e.g., planning, routing, tool invocation, and cross-agent summarization); thus, scores should be defined at the level of inter-agent states rather than tokens. **Schedule- and topology dependence.** In MAS, progress is schedule- and topology-dependent: the

value of an intermediate state depends on who acts next and what operation they perform (e.g., review, summarize, vote, aggregate). Even with identical agents, non-commutative operations make order matter; in single-agent reasoning chains, this dependence largely collapses because the next actor and operation are fixed. Heterogeneous agents. Beyond ordering, MAS agents can differ in role, tool access, system prompt, and even base model. Consequently, the same intermediate state can have a different expected value depending on the next agent's capabilities and interface. A PRM must be robust to changing agent identity and I/O surface, whereas single-agent chains keep the policy fixed across steps. Partial observability. In MAS, messages propagate over a communication graph, so each agent observes only a subset of the global state (in contrast to single-agent reasoning, which typically has access to the full prior chain). We therefore score each inter-agent state using only the information available to the acting agent at that moment, its locally visible intermediate state, so the value function remains well-defined under partial observability induced by the communication topology. These design choices draw on lessons from structured exploration (Wang et al., 2022; Yao et al., 2023; Snell et al., 2024) and verifierguided decoding (Cobbe et al., 2021; Lightman et al., 2023), while remaining compatible with implicit process signals learned from outcome-only data (Cui et al., 2025).

Contributions.

 We formulate MASPRM, a per-action, peragent process reward model that estimates the value of intermediate inter-agent states and acts as an inference time controller for MAS under fixed budgets.

- We present a search-generated supervision recipe that trains MASPRM from MAS-MCTS rollouts without manual step annotations while preserving progress sensitivity.
- We instantiate MASPRM-guided decoding via step-level beam search and value-guided MCTS over agent rollouts, improving decision quality and pruning unproductive intermediate inter-agent states early.

Key Results Relative to a single straight-through MAS pass (Greedy), our best MASPRM-guided configuration delivers large absolute accuracy gains; see Fig. 1 for the GSM8K compute/accuracy frontier. On GSM8K we observe a +30.7 point gain, and on MATH a +22.9 point gain.

2 Related Work

MAS optimization and agent reinforcement learning (RL). Recent MAS research optimizes communication graphs, roles, and tool routing to improve coordination and efficiency (Zhang et al., 2024; Zhou et al., 2025). Multi-agent reinforcement fine-tuning exposes instability under sparse rewards, underscoring the credit-assignment challenge (Liao et al., 2025). To mitigate delayed rewards, SPA-RL redistributes final rewards into stepwise contributions via a learned progress estimator and improves agent performance on interactive benchmarks (Wang et al., 2025). ARMAP automatically learns reward models from environment interaction (no human labels) and couples them with planning to evaluate trajectories and guide autonomous agents (Chen et al., 2025). Beyond these, LLM-as-judge methods enlist a centralized language-model critic to assign per-agent credit, either by generating dense agent-specific rewards from natural-language task descriptions (Lin et al., 2025) or by numerically decomposing team rewards into individualized signals (Nagpal et al., 2025), but recurring LLM inference introduces overheads that limit scalability for long inter-agent dialogues. In contrast, MASPRM serves as an efficient inference time controller: it scores messages and tool calls across the communication graph to steer multi-agent rollouts and provides per-agent progress signals.

PRM training and process supervision. PRMs provide dense, progress-aware feedback and have been used to guide search and prune low-promise branches (Setlur et al., 2024; Lightman et al.,

2023). To curb labeling cost, search-generated supervision with MCTS constructs step-level signals (ALPHAMATH ALMOST ZERO) (Chen et al., 2024); RSTAR-MATH pairs PRMs with MCTS to reach state-of-the-art math results (Guan et al., 2025); VERSAPRM trains multi-domain PRMs usable at inference (Zeng et al., 2025); and outcome-only training can yield implicit process rewards (Cui et al., 2025). For agents specifically, Process Reward Models for LLM Agents proposes AGENTPRM/INVERSEPRM, a practical framework for agent learning with process rewards (Choudhury, 2025); and automated process supervision (OMEGAPRM) scales PRM data collection for math (Luo et al., 2024). Unlike these, which largely target single-agent chains or domainspecific pipelines, we develop PRMs for MAS: our MASPRM scores inter-agent states to guide multi-agent search at inference and delivers dense, per-agent scores to stabilize collective optimiza-

3 Preliminaries

Problem and trajectories. Each instance consists of a question x and a hidden ground-truth answer y^* . An episode is a finite inter-agent dialogue that halts when a special "Final Answer" message is routed to a terminal node; correctness is evaluated only at termination.

Multi-agent communication graph. We model the system as a directed graph

$$G = (V \cup \{\mathbf{q}, \mathbf{sink}\}, E),$$

$$V = \{1, \dots, N\},$$

where every $i \in V$ is an agent, q is a non-acting question node that holds x, and sink is a non-acting terminal node with no outgoing edges. An edge $(i \rightarrow j) \in E$ denotes that i may route a message to j. Let the adjacency $A \in \{0,1\}^{(N+2)\times (N+2)}$ satisfy $A_{ij} = 1$ iff $(i \rightarrow j) \in E$. For $u \in V \cup \{q, sink\}$ define

$$\mathcal{N}_{\text{in}}(u) = \{ v : (v \to u) \in E \},$$

$$\mathcal{N}_{\text{out}}(u) = \{ w : (u \to w) \in E \}.$$

Schedule and horizon. A deterministic schedule $\sigma:\{1,\ldots,T\}\to V$ specifies the agent at depth t; the agent $i_t=\sigma(t)$ produces the t-th response. The horizon T upper-bounds the number of agent turns.

States, actions, and transitions. Let H_{t-1} be the transcript after t-1 agent turns: an ordered list of triples (speaker, message, recipient) consistent with G. A state is

$$s_t = (x, H_{t-1}, i_t),$$

containing the question (x), the partial transcript, and the identity of the next agent. When i_t acts at s_t , it chooses an action $a_t \in \mathcal{A}_{i_t}(s_t)$, realized as a textual response together with a recipient $r_t \in \mathcal{N}_{\text{out}}(i_t)$, producing the child state via the deterministic constructor

$$s_{t+1} = \text{next}(s_t, a_t),$$

which appends (i_t, a_t, r_t) to the transcript and sets the next agent to $i_{t+1} = \sigma(t+1)$ if $r_t \neq \text{sink}$. The recipient r_t determines which messages are routed and visible to later agents, but it does not affect the identity of the next agent. If $r_t = \text{sink}$, the episode terminates.

Terminal reward and return. Let s_T be terminal and \hat{y} be the extracted final answer from the last message. Define the terminal reward

$$R(s_T) = \begin{cases} +1, & \hat{y} = y^*, \\ -1, & \hat{y} \neq y^*, \end{cases}$$

and R(s) = 0 for non-terminal s. For any state s and admissible action a,

$$V^{\star}(s) = \mathbb{E}[R(s_T) \mid s],$$

$$Q^{\star}(s, a) = \mathbb{E}[R(s_T) \mid s, a].$$

Policies and candidate proposals. Each agent i is paired with a policy $\pi^{(i)}(\cdot \mid s)$ that induces a proposal distribution over textual responses and valid recipients. During search, a finite candidate set $\mathcal{C}_t \subset \mathcal{A}_{i_t}(s_t)$ is obtained by sampling from $\pi^{(i_t)}$.

Policy likelihood (length-normalized log-likelihood). To compare against policy-only guidance, we use the length-normalized log-likelihood (Wu et al., 2016; Yang et al., 2018; Koehn and Knowles, 2017)

$$\psi_{\text{pol}}(a \mid s_t) = \frac{1}{L} \sum_{\ell=1}^{L} \log p_{\theta}(w_{\ell} \mid w_{<\ell}, s_t), (1)$$

where $w_{1:L}$ are the generated tokens for action a. This single scalar can rank candidates.

Process value head. A process value head V_{ϕ} : $\mathcal{S} \rightarrow [-1,1]$ maps any (intermediate) state to its predicted expected terminal reward. Because s encodes the next agent, we interpret V_{ϕ} as a peragent, per-step local value: for an edge (s_t, a_t) with agent i_t , the local value of i_t 's decision is

$$V_{\phi}(\operatorname{next}(s_t, a_t)).$$

When referring to an agent node v acting at depth t, we write $V_{\phi}(v)$ as shorthand for $V_{\phi}(\operatorname{next}(s_t, a_t))$, i.e., the value of the post-action state immediately after v's message.

MCTS bookkeeping. For each visited edge (s,a) we maintain a visit count $N(s,a) \in \mathbb{N}$ and a running value sum $W(s,a) \in \mathbb{R}$ with empirical estimate

$$\hat{Q}(s,a) = \frac{W(s,a)}{\max\{1, N(s,a)\}}.$$

Selection uses the upper confidence bound for trees (UCT) (Kocsis and Szepesvári, 2006) with constant $c_{\rm UCT} > 0$:

$$a^{\star} = \arg \max_{a \in \mathcal{A}_{i_t}(s_t)} \left\{ \hat{Q}(s_t, a) + c_{\text{UCT}} \sqrt{\frac{\ln(1 + \sum_b N(s_t, b))}{1 + N(s_t, a)}} \right\}. \tag{2}$$

All successors must respect A and the schedule σ .

ORM. An ORM Υ maps a terminal pair (x, \hat{y}) to [-1, 1] and is only defined on terminal states. It is not used on intermediate states.

Notation for budgets. We use N simulations per instance (expansion budget), D the depth cap, and C_{\max} the per-node candidate cap.

4 MASPRM

Overview. MASPRM is a process reward model that supplies per-step, per-agent value estimates via a shared head V_{ϕ} . It is trained from search-generated supervision constructed by MAS-specific MCTS; no manual annotations are required. The same UCT rule in Eq. (2) is used both during label generation (training) and for inference-time search. An overview of MASPRM is shown in Fig. 2.

4.1 MASPRM training

MCTS phases (training). For each instance, MAS-MCTS proceeds with the standard four phases, all constrained by A and σ :

(i) Selection. Starting at the root state, repeatedly choose actions by UCT (2) until reaching a frontier

state. A state is a frontier state if and only if it is terminal or not yet fully expanded under the current candidate cap.

- (ii) Expansion. If the frontier state s_t is non-terminal, sample a candidate set $\mathcal{C}_t \subset \mathcal{A}_{i_t}(s_t)$ from $\pi^{(i_t)}$ and, for each $a \in \mathcal{C}_t$, create the child $s' = \operatorname{next}(s_t, a)$. We omit virtual visit initialization during training to avoid biasing Monte Carlo targets used for supervision.
- (iii) Evaluation (ground truth only). Continue selection/expansion until a terminal leaf s_T is reached, and set the leaf value

$$v_{\text{leaf}}(s_T) = R(s_T) \in \{-1, +1\},\$$

which corresponds to $\lambda=1$ in the unified rule of Eq. (3).

(iv) Backpropagation. For every edge (s, a) on the selected path, update

$$N(s, a) \leftarrow N(s, a) + 1,$$

$$W(s, a) \leftarrow W(s, a) + v_{\text{leaf}}(s_T),$$

$$\hat{Q}(s, a) = \frac{W(s, a)}{N(s, a)}.$$

A concise summary appears in Algorithm 1 (App. D).

Edge to child conversion and regression targets. After completing rollouts, for each visited edge (s,a) with child $s'=\operatorname{next}(s,a)$, define the process-level target

$$y_{\text{proc}}(s') \triangleq \hat{Q}(s, a) \in [-1, 1],$$

which is a Monte Carlo estimate of $Q^\star(s,a)$ backed up from terminal rewards. Collect $\mathcal{D}_{\mathrm{proc}}=\{(s',y_{\mathrm{proc}}(s'))\}$ over all edges and fit the process value head V_ϕ offline via

$$\min_{\phi} \frac{1}{|\mathcal{D}_{\text{proc}}|} \sum_{(s',y) \in \mathcal{D}_{\text{proc}}} \ell(V_{\phi}(s'), y),$$

with a bounded convex loss ℓ (e.g., Huber). The head output is range-restricted to [-1,1].

Outcome-only dataset and objective. Independently of $\mathcal{D}_{\mathrm{proc}}$, we extract a terminal dataset

$$\mathcal{D}_{\text{out}} = \{ (x, \hat{y}(s_T), r) : s_T, \quad r = R(s_T) \in \{-1, +1\} \}.$$

We then fit the ORM Υ_{θ} by

$$\min_{\theta} \ \frac{1}{|\mathcal{D}_{\text{out}}|} \sum_{(x,\hat{y},r) \in \mathcal{D}_{\text{out}}} \ell(\Upsilon_{\theta}(x,\hat{y}), r),$$

again using a bounded convex loss (e.g., Huber), with Υ_{θ} range-restricted to [-1,1]. At inference, the ORM is optionally used only at terminal leaves (see Eq. (3)).

4.2 Inference-time guidance

Leaf initializer and terminal mixing. We use two standard knobs: (i) a leaf initializer f_{INIT} for first-visit child nodes, and (ii) a single mixing coefficient $\lambda \in [0,1]$ applied only when a terminal signal is available. On the first visit to a frontier child $s' = \text{next}(s_t, a)$ we may set a virtual visit by

$$N(s_t, a) \leftarrow 1,$$

 $W(s_t, a) \leftarrow f_{\text{INIT}}(s_t, a),$
 $\hat{Q}(s_t, a) \leftarrow f_{\text{INIT}}(s_t, a),$

with $f_{\text{INIT}}(s_t, a) = V_{\phi}(s')$ (MASPRM initializer) or $f_{\text{INIT}}(s_t, a) = \psi_{\text{pol}}(a \mid s_t)$ (mean token log-likelihood). Leaf evaluation uses a single unified rule:

$$v_{\mathrm{leaf}}(s) = \begin{cases} R(s), \\ \text{training and } s \text{ terminal (we set } \lambda = 1), \\ (1 - \lambda) \, V_{\phi}(s) \, + \, \lambda \, \Upsilon \big(x, \hat{y}(s) \big), \\ \text{inference with ORM and } s \text{ terminal,} \\ V_{\phi}(s), \\ \text{otherwise (inference default } \lambda = 0). \end{cases} \eqno(3)$$

MCTS phases (inference). (i) Selection. From the root, traverse by UCT using the current \hat{Q} estimates.

- (ii) Expansion. At the first visit to a frontier non-terminal state s_t , sample \mathcal{C}_t from $\pi^{(i_t)}$; for each $a \in \mathcal{C}_t$, create $s' = \operatorname{next}(s_t, a)$ and initialize a virtual visit with $f_{\text{INIT}}(s_t, a) = V_\phi(s')$ unless otherwise stated.
- (iii) Evaluation. When a simulation stops at s (terminal), apply Eq. (3). We set λ =0 by default (pure bootstrap).
- (iv) Backpropagation. Update (N, W, \hat{Q}) along the traversed path exactly as in training: $N \leftarrow N+1$, $W \leftarrow W + v_{\text{leaf}}$, $\hat{Q} = W/N$. A final transcript is decoded by repeatedly choosing, from the root downward, the action with maximal \hat{Q} among available children. We summarize the inference time procedure in Algorithm 2 (App. D).

Step-level beam search (SBS). At depth t the acting agent i_t expands each beam state $s \in \mathcal{B}_t$ by sampling B_2 candidates from $\pi^{(i_t)}(\cdot \mid s)$ and scoring each successor by

$$score(a \mid s) = V_o(next(s, a)),$$

(or by $\psi_{pol}(a \mid s)$ for policy-only guidance). We pool all $|\mathcal{B}_t| B_2$ successors and retain the top- B_1 by score to form the next beam \mathcal{B}_{t+1} , repeating until a terminal enters the beam or t = T. We return the terminal path with the highest final state value. The algorithm 3 (App. D) summarizes the SBS we use.

5 Experiments & Results

Research Questions (RQ). We design our experiments to answer the following questions:

RQ1: MASPRM vs. policy-only at inference. Does a MASPRM improve accuracy under matched compute?

RQ2: MASPRM vs. ORM. How does MASPRM guidance compare to ORM, and are their gains complementary when combined?

RQ3: **Zero-shot out-of-distribution (OOD) gen- eralization.** Does a MASPRM trained on one dataset transfer zero-shot to another and improve EM at matched compute?

5.1 Overall experimental setup

In our experiments, we train MASPRM using the Qwen2.5-1.5B pretrained model. For the multiagent system, we adopt the architecture described in App. C, where each agent is instantiated with a Qwen2.5-1.5B-Instruct model. We evaluate our method on GSM8K (Cobbe et al., 2021) and MATH (Hendrycks et al., 2021) using exact match (EM) accuracy. Training supervision is obtained from MAS-MCTS rollouts with N=40 simulations and UCT constant $c_{\text{UCT}} = 4.0$, with leaf mixing $\lambda=1$ (so $v_{\text{leaf}}(s_{\ell})=R(s_{\ell})$), producing process-level value targets in [-1, 1] without manual annotation. Throughout, when we say policy likelihood baselines, the baseline scores candidates by the length-normalized log-likelihood as defined in Eq. (1); we use ψ_{pol} as a single scalar for ranking and (when applicable) initialization.

The MASPRM uses a tanh regression head and Huber loss, trained on separator tokens with 4-bit QLoRA (Dettmers et al., 2023) (rank 256, dropout 0.05) for 5 epochs, learning rate 1×10^{-5} , and gradient accumulation of 16. At inference, we compare settings at matched agent-call (AC) budgets; MASPRM calls and tokens are reported separately via MC and Tok, respectively: (i) Greedy decoding, (ii) Maj@5 (majority vote over k=5 independently sampled full MAS runs), (iii) SBS with either MASPRM scoring or policy likelihood, and

(iv) MASPRM-guided MCTS with N=20 simulations and at most 3 children per node. Candidate generation respects the MAS graph; SBS ranks partial solutions with the chosen scorer; MCTS uses $\lambda=0$ (unless stated); decoding proceeds greedily from the root by repeatedly selecting the child with maximal \hat{Q} .

Accounting and budget matching. We report: EM; AC = average number of agent calls (LLM)generations) per problem; MC = average number of MASPRM calls per problem (i.e., the average number of times the MASPRM is invoked); and Tok = average number of generated tokens perproblem. Let D denote the scheduled depth (number of agents that act once each). In our fixed 4-agent schedule, a single straight-through MAS pass uses AC = D = 4 (one call per agent). If MASPRM scoring is applied once per produced message, this pass also uses MC = 4. For SBS with global beam B_1 and per-state samples B_2 , $AC = B_2 + (D-1)B_1B_2$ (e.g., $B_2=5$, $B_1=3$, $D=4 \Rightarrow AC = 50$), but the number of AC in MCTS rollouts is not deterministic.

Evaluation protocol. The Verifier outputs Final Answer: <value> (see App. C). We extract the value with the regex Final Answer: (.*) and apply the normalization in App. B. We use a random seed and report single run metrics.¹

Baselines and variants. Maj@5 selects the plurality answer among 5 independent full MAS runs; ties are broken by highest aggregate length-normalized log-likelihood of the final answer. Maj@5 (+MASPRM step weights) weights each run's vote by $w = \frac{1}{T} \sum_{t=1}^T V_\phi(s_t)$ (mean MASPRM score across the path). +ORM end appends a learned ORM Υ (Qwen2.5-1.5B) that scores $(q, \text{final answer}) \mapsto [-1, 1]$ after decoding (tanh head similar to MASPRM); selection is by top- Υ among candidates.

Sampling settings. Decoding and search hyperparameters are in App. C (Decoding Settings) and App. B (Search configurations).

Hardware. Experiments run on 8× NVIDIA Tesla V100-PCIE-32GB (32 GB VRAM; driver 535.54.03; CUDA 12.2), an Intel Xeon Gold 6140 CPU @ 2.30 GHz, and 754 GB RAM.

 $^{^{1}}$ Max decode tokens per agent: $L_{\text{max}} = 1024$; see App. C.

5.2 A. MASPRM improves MAS inference under matched budgets

Evaluation. We evaluate whether process-level guidance improves multi-agent inference under fixed compute (Q1). All methods share the same MAS graph and schedule (Sec. 3) and are compared at matched AC budgets. We report EM, average AC per problem, average MC per problem, and average Tok per problem. Baselines include Greedy, Maj@5 (five independent full MAS runs; with our 4-agent schedule, this corresponds to 5D=20 agent calls), step-level beam search (SBS) with either policy likelihood scoring (length-normalized log-likelihood) or MASPRM scoring, and MCTS with either policy likelihood or MASPRM guidance.

Table 1: MASPRM improves MAS inference at matched compute. Abbreviations: AC=average agent calls per problem; MC=average MASPRM calls per problem; Tok=average generated tokens per problem; Maj@5: majority vote over 5 independent full MAS runs (uses $5 \times D = 20$ agent calls with D = 4). Notation B_1/B_2 indicates (global beam / per-state samples).

Method	EM↑ (%)	AC	MC	Tok↓
Greedy	43.9	4	0	1.6k
Maj@5	59.7	20	0	8.2k
SBS (policy likelihood) 1/5	53.9	20	0	8.1k
SBS (MASPRM) 1/5	57.1	20	20	8.2k
SBS (MASPRM) 3/5	65.4	50	50	17.3k
MCTS (policy likelihood), $N=20$	60.8	96	0	19.4k
MCTS (MASPRM), N=20	72.4	89	89	18.7k

Table 2: Same setup as GSM8K. Abbreviations: AC=average agent calls per problem; MC=average MASPRM calls per problem; Tok=average generated tokens per problem; Maj@5: majority vote over 5 independent full MAS runs. Notation B_1/B_2 indicates (global beam / per-state samples).

Method	EM↑ (%)	AC	MC	Tok↓
Greedy	25.1	4	0	1.2k
Maj@5	36.0	20	0	5.6k
SBS (policy likelihood) 1/5	34.8	20	0	5.5k
SBS (MASPRM) 1/5	39.7	20	20	5.8k
SBS (MASPRM) 3/5	41.1	50	50	12.5k
MCTS (policy likelihood), $N=20$	35.8	96	0	16.4k
MCTS (MASPRM), $N=20$	47.3	96	96	15.0k

Observation. On GSM8K (Table 1), at matched AC = 20 MASPRM-guided SBS improves EM from 53.9% to 57.1% (+2.2) with similar tokens (8.1k vs. 8.2k). Increasing beam size (SBS 3/5) reaches 65.4% at AC = 50, surpassing **Maj@5** (59.7%) by +5.7. With N=20 simulations, MCTS (MASPRM) attains 72.4%, exceeding MCTS (policy likelihood) at 60.8% by +11.6 while using fewer agent calls (89 vs. 96) and fewer tokens (18.7k vs. 19.4k). On MATH (Table 2), at matched

AC = 20 MASPRM-guided SBS increases EM from 34.8% to 39.7% (+4.9) with comparable tokens (5.5k vs. 5.8k), and SBS 3/5 reaches 41.1% at AC = 50 (+5.1 over Maj@5 at 36.0%). For MCTS with N=20 simulations, MASPRM yields 47.3% versus 35.8% for policy likelihood (+11.5) at the same AC (96) and fewer tokens (15.0k vs. 16.4k).

5.3 B. MASPRM guidance vs. ORM

Evaluation. We compare process-level guidance during search (MCTS MASPRM), an outcome model used at leaves with backup (MCTS +ORM end; leaves are evaluated by Υ and backed up), and their combination under identical search budgets. For completeness, we also evaluate vote-based reranking variants.

Table 3: MASPRM guidance vs. ORM (matched AC). ORM Υ details in App. B.

Method	GSM8K EM↑ (%)	MATH EM↑ (%)
MCTS (policy likelihood)	60.8	35.8
MCTS (MASPRM)	72.4	47.3
MCTS (+ORM end)	65.3	38.3
MCTS (MASPRM) + ORM	74.6	48.0
Maj@5	59.7	36.0
Maj@5 (+MASPRM step weights)	63.8	38.4
Maj@5 (+ORM end)	61.4	37.6

Observation. On GSM8K, MCTS (MASPRM) + ORM achieves 74.6% EM, a +30.7 point gain over Greedy (43.9%). Relative to MCTS(policy likelihood) at 60.8%, MASPRM-in-search adds +11.6 points (to 72.4%), and ORM-only yields 65.3%; the combination provides a further +2.2 over MASPRM alone. On MATH, MCTS (MASPRM)+ORM reaches 48.0% EM, a +22.9 point gain over Greedy (25.1%); MASPRM alone attains 47.3% and ORM-only 38.3%, with the combination adding +0.7 over MASPRM alone.

5.4 C. Zero-shot OOD transfer without retraining

Evaluation. We test whether a MASPRM trained on GSM8K transfers to MATH without retraining. We compare a policy-only search baseline, the frozen OOD MASPRM, and an in-distribution MASPRM (reference). All runs use the same MAS graph, policy, and matched #AC.

Observation. At closely matched budgets (AC \approx 94-96; tokens \approx 15k), a MASPRM trained on GSM8K transfers zero-shot to MATH with 44.2% EM, which is **+8.4** points over MCTS(policy likelihood) without MASPRM (35.8%) and within **3.1** points of the in-distribution MASPRM (47.3%).

Table 4: Zero-shot transfer of a GSM8K-trained MASPRM. Abbrev.: AC=average agent calls/problem; MC=average MASPRM calls/problem; Tok=average generated tokens/problem. The OOD MASPRM is frozen and not re-tuned.

Guidance	EM↑ (%)	AC	MC	Tok↓
MCTS (policy likelihood), no MASPRM	35.8	96	0	16.4k
OOD MASPRM (frozen)	44.2	94	94	15.3k
In-distribution MASPRM (reference)	47.3	96	96	15.0k

6 Discussion

Finding 1 — MASPRM-guided inference beats policy-only at matched compute. GSM8K and MATH, MASPRM-guided inference (SBS MASPRM and MCTS MASPRM) reliably outperforms matched policy-only baselines (Greedy, Maj@5, SBS policy likelihood, MCTS policy likelihood) at the same #AC; see the Observation in Sec. 5.2 and Tables 1 and 2. This supports our central claim that process-level signals are better aligned with multi-step, multiagent decision making than token likelihoods alone. Reporting MC separately clarifies overhead: improvements are achieved under matched agent-call budgets, with MASPRM evaluations acting as lightweight controllers (wall-clock comparison is in App. B.9) over the same action budget.

Finding 2 — Process guidance and outcome scoring are complementary. The comparison in Sec. 5.3 (Table 3) shows that using the MASPRM during search (process-level guidance) outperforms ORM when compute is matched. Moreover, combining the two (MASPRM in search + ORM at the end) yields the strongest accuracies among the variants considered.

Finding 3 — Progress signals transfer: OOD gains at matched compute. Sec. 5.4 demonstrates that a MASPRM trained on GSM8K transfers zero-shot to MATH and improves EM over a no MASPRM baseline at identical compute (Table 4). While an in-distribution MASPRM remains the upper bound, the OOD MASPRM narrows the gap, indicating that progress-sensitive signals learned from MAS-MCTS supervision capture reusable structure (e.g., step validity, simplification quality, verifier alignment) beyond a single dataset.

7 Conclusion & Future Work

We presented MASPRM, a per-action, per-agent process reward model that scores intermediate interagent states and steers inference-time search, improving accuracy at matched compute while acting as a drop-in controller for existing multi-agent workflows. Because many day-to-day MAS already coordinate planners, solvers, retrievers, tool routers, and verifiers (e.g., collaborative coding, customer support triage, and planning copilots), our approach can immediately make these systems more reliable and compute-aware without changing their base policies or requiring manual annotations. Looking ahead, we will (i) use MASPRM as a dense, fine-grained signal for multi-agent RL, both online and from logged traces, with safeguards against reward hacking; (ii) move beyond a fixed communication graph by using MASPRM to search for and/or learn the MAS topology and schedule, producing instance adaptive routing under explicit budget constraints; (iii) explore alternative objectives for the PRM beyond pointwise regression, including pairwise ranking, contrastive or advantage style (delta) targets, and distributional/uncertainty aware losses to improve calibration and robustness; and (iv) apply MASPRM across domains such as software engineering, retrieval augmented QA, robotics/planning, and multimodal agent teams, where process-level guidance can deliver practical gains under tight compute budgets.

References

- Guoxin Chen, Minpeng Liao, Chengxi Li, and Kai Fan. 2024. Alphamath almost zero: process supervision without process. *Advances in Neural Information Processing Systems*, 37:27689–27724.
- Zhenfang Chen, Delin Chen, Rui Sun, Wenjun Liu, and Chuang Gan. 2025. Scaling autonomous agents via automatic reward modeling and planning. *arXiv* preprint arXiv:2502.12130.
- Sanjiban Choudhury. 2025. Process reward models for llm agents: Practical framework and directions. *arXiv preprint arXiv:2502.10325*.
- Karl Cobbe, Vineet Kosaraju, Mohammad Bavarian, Mark Chen, Heewoo Jun, Lukasz Kaiser, Matthias Plappert, Jerry Tworek, Jacob Hilton, Reiichiro Nakano, and 1 others. 2021. Training verifiers to solve math word problems. *arXiv preprint arXiv:2110.14168*.
- Ganqu Cui, Lifan Yuan, Zefan Wang, Hanbin Wang, Wendi Li, Bingxiang He, Yuchen Fan, Tianyu Yu, Qixin Xu, Weize Chen, and 1 others. 2025. Process reinforcement through implicit rewards. *arXiv* preprint arXiv:2502.01456.
- Tim Dettmers, Artidoro Pagnoni, Ari Holtzman, and Luke Zettlemoyer. 2023. Qlora: Efficient finetuning of quantized llms. *Advances in neural information processing systems*, 36:10088–10115.
- Xinyu Guan, Li Lyna Zhang, Yifei Liu, Ning Shang, Youran Sun, Yi Zhu, Fan Yang, and Mao Yang. 2025. rstar-math: Small llms can master math reasoning with self-evolved deep thinking. *arXiv* preprint *arXiv*:2501.04519.
- Dan Hendrycks, Collin Burns, Saurav Kadavath, Akul Arora, Steven Basart, Eric Tang, Dawn Song, and Jacob Steinhardt. 2021. Measuring mathematical problem solving with the math dataset. *arXiv preprint arXiv:2103.03874*.
- Levente Kocsis and Csaba Szepesvári. 2006. Bandit based monte-carlo planning. In *European conference on machine learning*, pages 282–293. Springer.
- Philipp Koehn and Rebecca Knowles. 2017. Six challenges for neural machine translation. *arXiv preprint arXiv:1706.03872*.
- Junwei Liao, Muning Wen, Jun Wang, and Weinan Zhang. 2025. Marft: Multi-agent reinforcement fine-tuning. *arXiv preprint arXiv:2504.16129*.
- Hunter Lightman, Vineet Kosaraju, Yuri Burda, Harrison Edwards, Bowen Baker, Teddy Lee, Jan Leike, John Schulman, Ilya Sutskever, and Karl Cobbe. 2023. Let's verify step by step. In *The Twelfth International Conference on Learning Representations*.
- Muhan Lin, Shuyang Shi, Yue Guo, Vaishnav Tadiparthi, Behdad Chalaki, Ehsan Moradi Pari, Simon Stepputtis, Woojun Kim, Joseph Campbell, and Katia Sycara.

- 2025. Speaking the language of teamwork: Llmguided credit assignment in multi-agent reinforcement learning. *arXiv* preprint arXiv:2502.03723.
- Liangchen Luo, Yinxiao Liu, Rosanne Liu, Samrat Phatale, Meiqi Guo, Harsh Lara, Yunxuan Li, Lei Shu, Yun Zhu, Lei Meng, and 1 others. 2024. Improve mathematical reasoning in language models by automated process supervision. *arXiv* preprint *arXiv*:2406.06592.
- Kartik Nagpal, Dayi Dong, Jean-Baptiste Bouvier, and Negar Mehr. 2025. Leveraging large language models for effective and explainable multi-agent credit assignment. *arXiv* preprint arXiv:2502.16863.
- Amrith Setlur, Chirag Nagpal, Adam Fisch, Xinyang Geng, Jacob Eisenstein, Rishabh Agarwal, Alekh Agarwal, Jonathan Berant, and Aviral Kumar. 2024. Rewarding progress: Scaling automated process verifiers for llm reasoning. *arXiv preprint arXiv:2410.08146*.
- Charlie Snell, Jaehoon Lee, Kelvin Xu, and Aviral Kumar. 2024. Scaling llm test-time compute optimally can be more effective than scaling model parameters. *arXiv preprint arXiv:2408.03314*.
- Hanlin Wang, Chak Tou Leong, Jiashuo Wang, Jian Wang, and Wenjie Li. 2025. Spa-rl: Reinforcing llm agents via stepwise progress attribution. *arXiv* preprint arXiv:2505.20732.
- Xuezhi Wang, Jason Wei, Dale Schuurmans, Quoc Le, Ed Chi, Sharan Narang, Aakanksha Chowdhery, and Denny Zhou. 2022. Self-consistency improves chain of thought reasoning in language models. *arXiv* preprint arXiv:2203.11171.
- Yonghui Wu, Mike Schuster, Zhifeng Chen, Quoc V Le, Mohammad Norouzi, Wolfgang Macherey, Maxim Krikun, Yuan Cao, Qin Gao, Klaus Macherey, and 1 others. 2016. Google's neural machine translation system: Bridging the gap between human and machine translation. *arXiv* preprint arXiv:1609.08144.
- Yilin Yang, Liang Huang, and Mingbo Ma. 2018. Breaking the beam search curse: A study of (re-) scoring methods and stopping criteria for neural machine translation. *arXiv* preprint arXiv:1808.09582.
- Shunyu Yao, Dian Yu, Jeffrey Zhao, Izhak Shafran, Tom Griffiths, Yuan Cao, and Karthik Narasimhan. 2023. Tree of thoughts: Deliberate problem solving with large language models. *Advances in neural information processing systems*, 36:11809–11822.
- Thomas Zeng, Shuibai Zhang, Shutong Wu, Christian Classen, Daewon Chae, Ethan Ewer, Minjae Lee, Heeju Kim, Wonjun Kang, Jackson Kunde, and 1 others. 2025. Versaprm: Multi-domain process reward model via synthetic reasoning data. *arXiv preprint arXiv:2502.06737*.

Guibin Zhang, Yanwei Yue, Xiangguo Sun, Guancheng Wan, Miao Yu, Junfeng Fang, Kun Wang, Tianlong Chen, and Dawei Cheng. 2024. G-designer: Architecting multi-agent communication topologies via graph neural networks. *arXiv preprint arXiv:2410.11782*.

Han Zhou, Xingchen Wan, Ruoxi Sun, Hamid Palangi, Shariq Iqbal, Ivan Vulić, Anna Korhonen, and Sercan Ö Arık. 2025. Multi-agent design: Optimizing agents with better prompts and topologies. *arXiv* preprint arXiv:2502.02533.

A Illustrative Examples

A.1 Example MAS and schedule

The four-agent example (Fig. 3) is illustrative only and does not exactly match the experimental MAS; see App. C for the configuration used in the results. Dashed directed edges indicate admissible message routing; one agent acts per depth according to σ , producing outputs o_1, \ldots, o_4 .

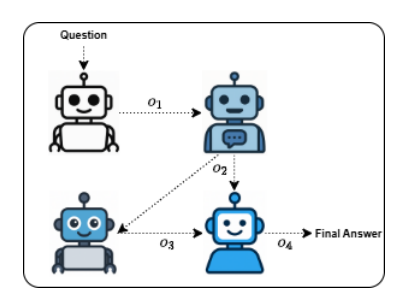


Figure 3: **Example MAS** (four agents) and schedule. Dashed directed edges define admissible routing and the order of agent outputs o_1 - o_4 ; one agent acts per depth according to σ .

A.2 Stylized transcript for a GSM8K-style problem

We visualize (Fig. 4) one rollout on the ticket question: "A group buys 14 tickets; adult \$5, child \$3; total \$56. How much more was spent on adult tickets than on child tickets?" The roles are *Reader & Fact Extractor* (o_1) , *Planner & Variable Setter* (o_2) , *Arithmetic Worker* (o_3) , and *Verifier & Finalizer* (o_4) . Two trajectories are shown: the green path solves a+c=14 and 5a+3c=56 to get a=c=7 and returns 5a-3c=35-21=14; the red path makes an arithmetic error and outputs 15.

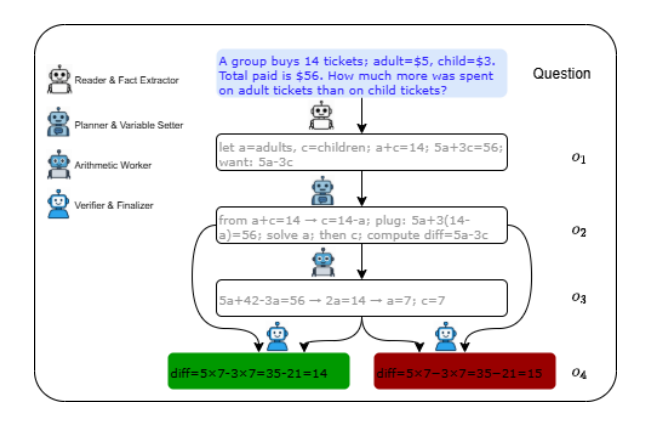


Figure 4: **Stylized transcript (example).** A 4-agent pipeline produces outputs o_1 - o_4 . Green is correct $(a=c=7 \Rightarrow 5a-3c=14)$; red is incorrect $(35-21 \neq 15)$.

A.3 MCTS rollout with MASPRM values

Fig. 5 shows value-guided search over the unrolled tree: internal annotations (e.g., 0.5, 0.25) depict example mean values \overline{V} backed up from MASPRM leaf evaluations; white circles denote agent outputs; green/red leaves indicate terminal reward +1/-1 (correct/incorrect). Selection uses UCT (Eq. 2).

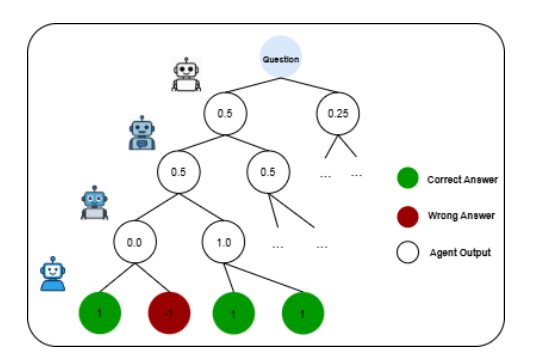


Figure 5: MCTS over the unrolled tree (example). Numbers on nodes are illustrative mean values \overline{V} ; green/red leaves denote $R \in \{+1, -1\}$.

B Additional Experimental Details

B.1 Datasets and splits

We use GSM8K and MATH. For each, validation is a random 5% split of the training set. We use the provided test sets and ensure no training leakage.

- **GSM8K:** 7,099 train, 374 validation, 1,319 test
- MATH: 9,975 train, 525 validation, 2000 test

B.2 Answer extraction and normalization

Final answers are extracted from the last agent via the regex Final Answer: (.*). Fallback: last numeric span in the final message. Preprocessing: lowercase; strip commas/spaces; remove units in {USD, dollars, \$}. Numeric tolerance $\delta=10^{-3}$. Non-parsable outputs or timeouts are scored incorrect.

B.3 MAS graph, prompts, and schedule

Roles and prompts are listed in App. C; schedule length D=4. Max decode tokens per agent $L_{\rm max}=1024$.

B.4 MASPRM training data generation

We run MAS-MCTS with N=40 simulations, $c_{\text{UCT}}=4.0$, $C_{\text{max}}=3$ children per expansion on training problems. Targets are clamped to $[-1+\epsilon,1-\epsilon]$ with $\epsilon=10^{-4}$ and used directly with

Huber loss on the \tanh -bounded outputs. Leaf values are set to the terminal reward (λ =1 in Sec. 3).

B.5 MASPRM model and optimization

Backbone: Qwen2.5-1.5B with a tanh head. QLoRA 4-bit, rank 256, dropout 0.05; batch size 8 (effective with grad accumulation 16); LR 1×10^{-5} ; epochs 5; optimizer *ADAMW*; weight decay 0.01. Evaluation metrics: Pearson, RMSE, MAE, R^2 , bias.

B.6 Search configurations

SBS: "1/5" means $(B_2, B_1) = (5, 1)$; "3/5" means (5, 3). Temperature = 0.7, top-p = 0.95. Tiebreaking by higher MASPRM score (if applicable), else by higher final-answer policy likelihood. MCTS: Selection uses UCT (Eq. 2); expansion samples up to $C_{\rm max} = 3$ children by top-p sampling from the current agent; leaf evaluation uses V_{ϕ} ($\lambda = 0$); rollout depth capped at D = 4; on dead ends, back up the current MASPRM leaf value. No policy priors are added to UCT unless otherwise stated.

B.7 ORM Υ

Training hyperparameters and optimizer mirror the MASPRM training, using a sequence classification head.

B.8 OOD transfer protocol

The GSM8K-trained MASPRM is frozen for MATH (no re-tuning); we keep the same normalization/clamping.

B.9 Wall-clock Comparison

Each AC takes 18.94 s on average, while each MC takes 0.16 s on average for GSM8K dataset.

C MAS Graph, Prompts, and Configuration

C.1 Agent roles, system prompts, and decoding

The multi-agent system (MAS) uses four specialized agents and a fixed schedule of one turn per agent (depth $D{=}4$): Reader \rightarrow Planner \rightarrow Solver \rightarrow Verifier.

```
- name: Reader
system_prompt: "You are the Reader.
Extract key facts and restate the question."
max_new_tokens: 1024
```

```
- name: Planner
system_prompt: "You are the Planner.
Propose a concise plan to solve the task."
max_new_tokens: 1024
- name: Solver
system_prompt: "You are the Solver.
Carry out the plan and compute results."
max_new_tokens: 1024
- name: Verifier
system_prompt: "You are the Verifier.
Double-check the result and output exactly:
Final Answer: <value>"
max_new_tokens: 1024
```

C.2 Communication edges and schedule

Edges are directed and -1 denotes the root (question). This replicates the connections used in all experiments:

```
# Edges (src, dst). Use -1 for ROOT (
... Question).
edges:
- [-1, 0] # Question -> Reader
- [-1, 1] # Question -> Planner
- [ 0, 1] # Reader -> Planner
- [ 1, 2] # Planner -> Solver
- [-1, 3] # Question -> Verifier
- [ 2, 3] # Solver -> Verifier
# Fixed schedule (one turn per depth):
schedule_order: [Reader, Planner, Solver,
... Verifier]
```

C.3 Decoding and search settings (for reproducibility)

Unless specified otherwise in the main text, decoding and search use:

```
Decoding Settings

temperature: 0.7
top_p: 0.95
max_new_tokens_per_agent: 1024
```

D Algorithms (Brief Overview)

This appendix summarizes the procedures used for training-time data generation, inference time MCTS, and step-level beam search. The descriptions are intentionally brief and omit implementation details not essential for understanding the method.

Algorithm 1 MAS-MCTS Training Data Generation (general)

```
Input: Instance (x, y^*); communication graph G; schedule \sigma; simulations N
  1: Initialize empty search tree with statistics N(s, a) = 0, W(s, a) = 0
 2: for k = 1 to N do
 3:
           s \leftarrow \operatorname{root}(x); path \leftarrow []

⊳ Selection

           while s is expanded and non-terminal do
 4:
               \begin{aligned} a \leftarrow \arg\max_{b} \left\{ \hat{Q}(s,b) + c_{\text{UCT}} \sqrt{\frac{\ln(1 + \sum_{u} N(s,u))}{1 + N(s,b)}} \right\} \\ \text{Append } (s,a) \text{ to path; } s \leftarrow \text{next}(s,a) \end{aligned}
 5:
 6:
           end while

    Expansion (no virtual visits in training)

 7:
 8:
           if s non-terminal then
                Sample a candidate set C from the current agent's policy \pi^{(i_t)}(\cdot \mid s)
 9:
10:
                For each a \in \mathcal{C}, create child s' = \text{next}(s, a)
           end if

    ▷ Evaluation with ground truth (terminal reward)

11:
12:
           Continue selection/expansion until reaching a terminal leaf s_T
13:
           v \leftarrow R(s_T) \in \{-1, +1\}
                                                       (corresponds to \lambda=1 during training)
                                                                                                                      ▶ Backpropagation
           for each (u, b) in path do
14:
                N(u,b) \leftarrow N(u,b) + 1; \quad W(u,b) \leftarrow W(u,b) + v; \quad \hat{Q}(u,b) \leftarrow \frac{W(u,b)}{N(u,b)}
15:
           end for
16:
17: end for
18: Process targets: For every visited edge (s, a) with child s' = \text{next}(s, a), set y_{\text{proc}}(s') \leftarrow \hat{Q}(s, a)
      and add (s', y_{\text{proc}}(s')) to \mathcal{D}_{\text{proc}}
19: Fit the process head: Train V_{\phi} on \mathcal{D}_{\text{proc}} with a bounded regression loss
```

Algorithm 2 Inference-Time MCTS with MASPRM (and optional ORM)

```
Input: Instance x; graph G; schedule \sigma; simulations N; optional ORM \Upsilon
  1: Initialize empty search tree with statistics N(s,a) = 0, W(s,a) = 0
 2: for k = 1 to N do
          s \leftarrow \operatorname{root}(x); path \leftarrow []

⊳ Selection

 3:
          while s is expanded and non-terminal do
 4:
               a \leftarrow \arg\max_{b} \left\{ \hat{Q}(s,b) + c_{\text{UCT}} \sqrt{\frac{\ln(1 + \sum_{u} N(s,u))}{1 + N(s,b)}} \right\}
 5:
               Append (s, a) to path; s \leftarrow \text{next}(s, a)
 6:
          end while
 7:
                                                                     \triangleright Expansion with virtual visit initialization from V_{\phi}
          if s non-terminal then
 8:
               Sample a candidate set C from \pi^{(i_t)}(\cdot \mid s)
 9:
               for each a \in \mathcal{C} do
10:
                    s' \leftarrow \text{next}(s, a)
11:
                    N(s,a) \leftarrow 1; \quad W(s,a) \leftarrow V_{\phi}(s'); \quad \hat{Q}(s,a) \leftarrow V_{\phi}(s')
12:
               end for
13:
          end if
                                         ▶ Leaf evaluation: bootstrap by default; use ORM at terminal if provided
14:
          if s is terminal and ORM is used then
15:
               v \leftarrow \Upsilon(x, \hat{y}(s))
                                                                                             (effective \lambda=1 at terminal leaves)
16:
17:
               v \leftarrow V_{\phi}(s)
                                                                                                          (default bootstrap; \lambda = 0)
18:
          end if
                                                                                                                 ▶ Backpropagation
19:
20:
          for each (u, b) in path do
               N(u,b) \leftarrow N(u,b) + 1; \quad W(u,b) \leftarrow W(u,b) + v; \quad \hat{Q}(u,b) \leftarrow \frac{W(u,b)}{N(u,b)}
21:
22:
          end for
23: end for
24: Decode: From the root, greedily follow at each depth the child with maximal \hat{Q}
```

Algorithm 3 Step-Level Beam Search (SBS) with MASPRM or Policy Score (B_1/B_2)

```
Input: Instance x; graph G; schedule \sigma; global beam B_1; per-state samples B_2; scorer f where f(s') \in
      \{V_{\phi}(s'), \psi_{\text{pol}}(a \mid s)\}
  1: Initialize beam \mathcal{B} \leftarrow \{ \operatorname{root}(x) \}
                                                               \triangleright D is the schedule length (one agent per depth); i_t = \sigma(t)
 2: for t = 1 to D do
 3:
           \mathcal{C}_{\text{all}} \leftarrow []
 4:
           for each s \in \mathcal{B} do
                Sample B_2 candidate actions \{a^{(b)}\}_{b=1}^{B_2} \sim \pi^{(i_t)}(\cdot \mid s)
  5:
                for b = 1 to B_2 do
  6:
                     s' \leftarrow \text{next}(s, a^{(b)}); \quad \text{score}(s') \leftarrow f(s')
                                                                                                                             (e.g., f = V_{\phi})
  7:
                     Append (s', score(s')) to C_{all}
 8:
 9:
                end for
           end for
10:
           \mathcal{B} \leftarrow \text{top-}B_1 \text{ states in } \mathcal{C}_{\text{all}} \text{ by score}

⊳ Global pool across parents

11:
           Early stop: If any s \in \mathcal{B} is terminal, optionally stop and return the best terminal by score
12:
13: end for
14: Select output: If no terminal in the final beam, select the highest-scoring state and finalize with the
      Verifier
```